ORIGINAL PAPER

Friction ridges in cockroach climbing pads: anisotropy of shear stress measured on transparent, microstructured substrates

Christofer J. Clemente · Jan-Henning Dirks · David R. Barbero · Ullrich Steiner · Walter Federle

Abstract The contact of adhesive structures to rough surfaces has been difficult to investigate as rough surfaces are usually irregular and opaque. Here we use transparent, microstructured surfaces to investigate the performance of tarsal euplantulae in cockroaches (*Nauphoeta cinerea*). These pads are mainly used for generating pushing forces away from the body. Despite this biological function, shear stress (force per unit area) measurements in immobilized pads showed no significant difference between pushing and pulling on smooth surfaces and on 1-μm high microstructured substrates, where pads made full contact. In contrast, on 4-μm high microstructured substrates, where pads made contact only to the top of the microstructures, shear stress was maximal during a push. This specific direction dependence is explained by the interlocking of the microstructures with nanometre-sized "friction ridges" on the euplantulae. Scanning electron microscopy and atomic force microscopy revealed that these ridges are anisotropic, with steep slopes facing distally and shallow slopes proximally. The absence of a significant direction dependence on smooth and 1-μm high microstructured surfaces suggests the effect of interlocking is masked by the stronger influence of adhesion on friction, which acts equally in both directions. Our findings show that cockroach euplantulae generate friction using both interlocking and adhesion.

Keywords Adhesion · Tribology · Biomechanics · Direction dependence · Lithography

Introduction

Many insects, spiders and some vertebrates are capable of climbing and walking upside down on diverse substrates, using adhesive structures on their legs (Scherge and Gorb 2001). They are adapted for climbing on natural substrates such as plant or rock surfaces, which are often rough, showing differences in height over many different length scales. Despite this, most studies on animal adhesion have focused on smooth surfaces (Jiao et al. 2000; Gorb 2001; Gorb et al. 2001; Federle et al. 2002; Drechsler and Federle 2006; Bullock et al. 2008).

The reason for this bias is simple; it is difficult to visualize the adhesive contact on rough surfaces. Previous studies of animal attachment to rough substrates have used different types of normal or abrasive paper, cloth or natural plant surfaces, or replicas of these surfaces, which are all irregular and opaque (Stork 1980; Lees and Hardie 1988; Betz 2002; Santos et al. 2005; Drechsler and Federle 2006; Huber et al. 2007; Gorb 2008; Voigt et al. 2008; Bullock and Federle 2009). In these studies, the detailed properties of the surfaces were mostly unknown, and the lack of transparency made it impossible to assess whether and how

C. J. Clemente (✉) · J.-H. Dirks · W. Federle
Department of Zoology, University of Cambridge,
Downing Street, Cambridge CB2 3EJ, UK
e-mail: cc498@cam.ac.uk

D. R. Barbero · U. Steiner
Department of Physics, Nanoscience Centre,
Cavendish Laboratory, J J Thomson Avenue,
Cambridge CB3 0HE, UK

U. Steiner
Freiburg Institute for Advanced Studies (FRIAS),
University of Freiburg, Albertstr. 19,
79104 Freiburg, Germany

changes in adhesion and friction depended on changes in contact area.

The interaction of adhesives with rough surfaces is of obvious commercial importance and has been the subject of numerous theoretical studies (Fuller and Tabor 1975; Hui et al. 2001; Kendall 2001; Hui et al. 2005; Peressadko et al. 2005; Kim and Bhushan 2007; Persson 2007a). As biological attachment systems have evolved the ability to make contact with diverse substrates of different surface roughness, it is hoped that they can inspire the design of novel adhesives that provide controllable contact to both smooth and rough substrates. However, the detailed mechanisms of how they adapt to the surface topography are still unclear. To clarify these mechanisms, it is necessary to study the performance of natural adhesive pads on rough substrates under controlled conditions. Recent developments in lithographic methods have made it possible to fabricate highly regular surface patterns with various sizes, shapes and chemical properties. These substrates are not only characterized by a well-defined surface "roughness" but they can also be made from transparent materials. In this study, we measure both friction and contact area on a microstructured, transparent surface to investigate how insect adhesive structures interact with rough surfaces.

To evaluate this new approach, we selected a climbing pad with a microscopic surface structure that suggested direction-dependent friction, the tarsal euplantulae of the cockroach *Nauphoeta cinerea*. We recently discovered the euplantulae in this species are friction pads mainly used for generating pushing forces during locomotion (Clemente and Federle 2008). While attachment organs on the distal pretarsus (claws and arolium) are effective at pulling and generating adhesion during vertical climbing or inverted walking, insect foot tips are ill-suited for pushing because of the flexibility of the segmented tarsus. As a consequence, the cockroach arolium and the euplantulae were found to have an opposite direction dependence. When the tarsus was free to move, the arolium generated the highest friction when pulling, while the euplantulae did so when pushing. On the investigated smooth glass substrate, this direction dependence was only caused by changes in contact area but not in shear stress (Clemente and Federle 2008).

On rough surfaces, attachment organs must also be able to push and pull. Most insects have claws on the pretarsus, which provide a grip by interlocking with larger surface asperities (Betz 2002; Dai et al. 2002; Endlein and Federle 2008; Voigt et al. 2008). Due to their distal location and hook-like structure, claws are used for pulling. Apart from some distally directed hairs and spines on the tarsus and tibia (Spagna et al. 2007), there is no functional "pushing" equivalent of the claws, suggesting that the euplantulae must be able to push both on smooth and rough surfaces.

Could the tarsal euplantulae of cockroaches be designed for effective pushing on rough surfaces? Scanning electron microscopy showed that the surface of the euplantulae is covered by a regular pattern of oblong 'platelets' separated by small transverse ridges, which have a steeper slope on the distal side (Clemente and Federle 2008). This design could facilitate interlocking with a rough substrate during a pushing stride.

In this study, we investigate the mechanism of euplantula direction-dependence by measuring friction and contact area on a smooth and a microstructured, transparent substrate.

Methods

Study animals

Adult cockroaches (*N. cinerea*, Blaberidae; body mass 488 ± 19 mg; mean $\pm$ SE, $n = 30$) were taken from a laboratory colony kept in plastic containers at 24°C. Cockroaches were fed dog food and water ad libitum.

Scanning electron microscopy (SEM)

Tarsi from adult cockroaches were cut and immediately transferred into fixative (4% glutaraldehyde in 0.1 M PIPES buffer at pH 7.4) for 48 h at 4°C, washed with deionized water and dehydrated in 100% ethanol. Samples were mounted on SEM stubs, sputter-coated with 20 nm gold, and examined in a FEI XL30-FEG scanning electron microscope at 10 kV.

Atomic force microscopy (AFM)

The three-dimensional topography of the euplantula surface of *N. cinera* was investigated using a Dimension 3100 atomic force microscope (AFM) in 'tapping mode' (Nanoscope software, NSG 10 tips, NT MDT, $D = 11.5$ N/m). AFM was performed on one tarsus that was fixated and gold-coated as for SEM. The surface profile was measured at two different positions of two euplantulae on the second and third tarsal segment as indicated in Fig. 1b. After imaging an area of 10×10 μm for overview, we adjusted the scanning direction so that it was perpendicular to the ridges (scanning velocity 13 μm/s, 512 samples/10 μm). Cross sections of the data were manually selected, corrected for tilt in MATLAB (The Mathworks Inc.) and manually analysed to obtain ridge height, width and incline.

Interference reflection microscopy (IRM)

IRM was used to characterize the surface contact of the euplantulae and to observe the effect of the ridges on fluid distribution under the euplantulae. *N. cinerea* legs were
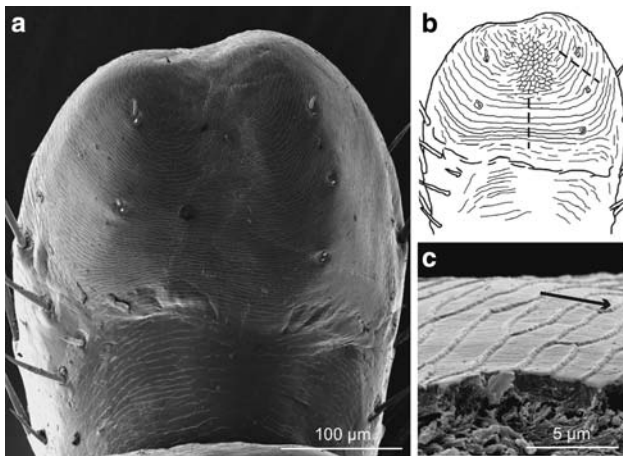
Fig. 1 a Distal euplantula, from the hindleg tarsus of *N. cinerea*. **b** Schematic of a single euplantula of *N. cinerea* showing the orientation of the ridges. *Dashed lines* indicate the position of the medial and the lateral AFM scans. **c** SEM freeze fracture of the anisotropic surface sculpture of the euplantulae, *arrow* indicates distal direction

fixed with dental cement (ESPE Protemp II, 3M) and the euplantulae were pressed against a smooth glass cover slip. Pads were held in contact for 4 min, to allow the fluid to build up in the contact area. Images were taken with a monochromatic illumination (546 nm, illuminating numerical aperture 1.25) using a Leica DRM Microscope and a QICAM 12-bit monochrome camera.

Fabrication of microstructured, transparent PMMA test substrates

A solution of polymethylmethacrylate (PMMA) was prepared by dissolving PMMA powder (Mw = 330,000, Polymer Labs) in toluene. A thin film of PMMA was prepared by spin-coating the solution onto a clean glass slide. The cleaning procedure was as follows: the glass slide was cleaned in acetone for 30 min at 40°C with an ultrasonicator. This was repeated again in isopropanol under the same conditions, and then blown dried in a nitrogen atmosphere. The glass slide was then cleaned with a highly pressurized carbon dioxide snowjet to remove any dust and small particles that could have adhered onto the surface of the glass slide. Once the PMMA film was deposited onto the glass slide, the pillars were formed into the film by nanoimprinting from a microstructured ethylene tetrafluoroethylene (ETFE) mold. Details of this procedure and fabrication of the molds can be found in Barbero et al. (2007). The glass/PMMA substrate and the ETFE mold were placed in contact (without any additional pressure applied) and heated to ~150°C. Once a homogeneous temperature was reached, a pressure of ~20 bar was applied by a mechanical press (Obducat AB, Sweden) for several minutes to ensure complete filling of the mold by the PMMA. The assembly was

then cooled down to 40°C by an air cooling system mounted onto the press. The pressure was released, and the glass/PMMA substrate was separated from the ETFE mold. This procedure yielded a well defined 4×4 mm squared microstructured array of 4 μm diameter flat-topped pillars, with near vertical walls, spaced with 12 μm periodicity (Fig. 4a). Only the pillar height was varied between samples, with 1 and 4 μm high pillars included in the analysis. The surface energy of PMMA surfaces has been measured as 41–43 mN/m at 20°C (Jones and Richards 1999). The contact angle of water on PMMA is 76° (Busscher et al. 1984).

Single-leg force measurements

To measure friction forces of the euplantulae in *N. cinerea*, cockroaches were briefly anesthetized using CO_2 and fastened to a mount using parafilm tape. We used hind legs for all measurements. The fifth tarsal segment was held away from the surface and fixed using paraffin wax, imitating the natural walking posture of the tarsus in free walking cockroaches (Roth and Willis 1952; Frazier et al. 1999). The tarsal segments bearing the euplantulae (Ta1–Ta4) were fixed on their dorsal side using paraffin wax and dental cement.

Forces were measured using 2D bending beam consisting of two cut plates of carbon–manganese steel 0.30 mm thick, joined at right angles (Spring constant 452 N/m). Two mounted full bridges of 420 Ω semiconductor strain gauges (Micron Instruments, Simi Valley, CA) allowed force measurement, calibrated for different lever arm lengths by applying milligram weights and defined displacements. Euplantulae were brought into contact with either smooth PMMA (Spin-cast polymer films from good solvents have a surface roughness of 5–8 Å; Russell 1990) or a microstructured transparent surface, both attached to the end of the bending beam. Pad contact area was recorded under reflected light using a HotShot PCI 1280 B/W camera (NAC image technology) triggered at 10 Hz. Complete contact to the smooth or microstructured surface was indicated by a dark area in the reflected light image (Fig. 4b). Force input signals were amplified (GSV1T8, ME-Systeme) and recorded to a data acquisition board (PCI-6035E, National Instruments) with a sampling frequency of 1,000 Hz. The force transducer was mounted on a computer-controlled 3D positioning stage (M-126PD, C-843, Physik Instrumente). Motor movements, video trigger and force recording were synchronized by a custom-made LabVIEW program (National Instruments) that included a normal force feedback mechanism (frequency 50 Hz).

Before a friction measurement, the pad was brought into contact with the glass plate for 2 s with a normal force of either 0.5 or 1.0 mN, using force feedback. Sliding

movements covering 2 mm were performed with a velocity of 0.1 mm/s either in the proximal direction (imitating the leg pulling towards the body) or in the distal direction (imitating the leg pushing away from the body). The normal force was kept constant during each slide via force feedback. We used the maximum friction force of each slide for further analysis. Results for all analyses are presented as mean ± standard error.

Results

Morphology

The general morphology of the tarsus, arolium and euplantulae of *N. cinerea* cockroaches has been described previously (Clemente and Federle 2008). The first four tarsomeres bear soft, pad-like structures, called euplantulae, on their ventral side. The epicuticular surface of the euplantulae is regularly patterned by oblong 'platelets', separated by small ridges (Fig. 1a). SEM images suggested that the distal-facing edge of these ridges is steeper than the proximal-facing edge, giving the impression that each platelet overlaps the one distal to it (Fig. 1c). The ridges in the midline of the euplantulae run transversely. However, the ridges turn distally by ca. 45° towards the lateral sides of the pad (Fig. 1b), producing a regular pattern of curved lines reminiscent of the friction ridges on human fingertips.

Atomic force microscopy confirmed the asymmetry of the ridges (Fig. 2a, c). The distal sides of the ridges were significantly steeper than the proximal sides (paired t test for maximal inclines, $t_{14} = 2.14$, $P = 0.003$, $N = 15$), with the steepest ridge having a slope of 70°. The mean height for all ridges was 184 ± 21 nm, however, the lateral ridges were significantly higher than the medial ridges (lateral ridge height = 221 ± 24 nm, $n = 10$; medial ridge height 110 ± 10 nm, $n = 5$; $t_{12} = 2.18$, $P = 0.001$).

IRM showed that the euplantula cuticle is able to make full contact to a smooth surface despite the presence of surface ridges. This may be achieved by the conformability of the soft cuticle and by the secretion of fluid, which can fill up the gaps in between the ridges. The fluid secretion of the euplantulae is two-phasic and consists of volatile, hydrophilic droplets (fluid A, appearing bright with high-contrast fringes in IRM) dispersed in a hydrophobic fluid (fluid B, appearing darker with weak fringe contrast in IRM), similar to previous findings for ants and stick insects (Federle et al. 2002). However, the amount of fluid B present in the euplantulae appears to be very small. Even after several minutes in contact with glass, only one (low-contrast) interference fringe became visible at the edge of the contact zone. The volume of fluid was much smaller than that observed at the edge of arolia in ants and stick insects
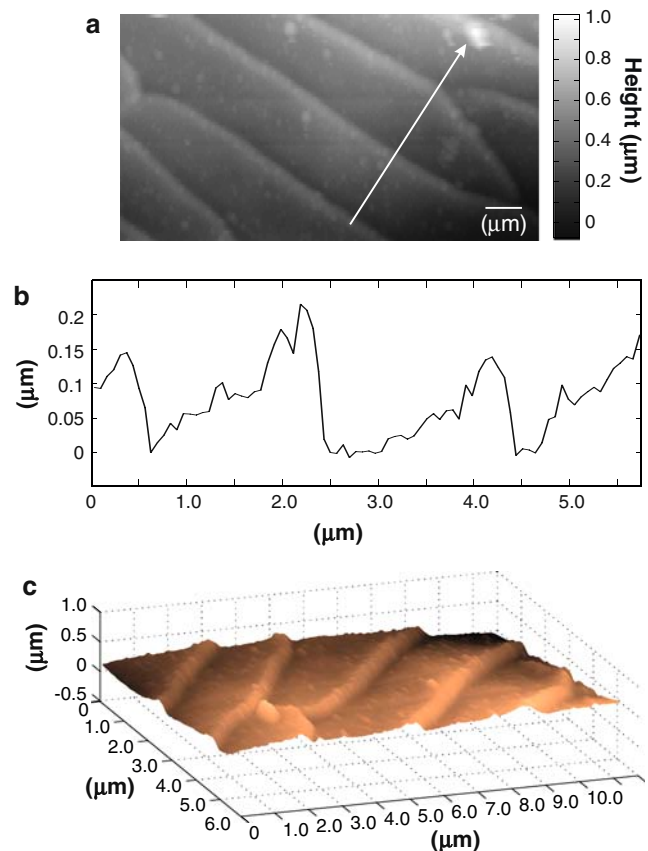

Fig. 2 **a** AFM scan of the euplantula surface. The regular ridge pattern is oriented perpendicularly to the proximal–distal axis of the leg. The *white arrow* indicates the distal direction and the position of the height profile. **b** Height profile along the *arrow* shown in **a**. **c** 3D view of the AFM scan shown in a. All scales are in µm

(Federle et al. 2002). In IRM images, the minute surface ridges were visible by the disruption of fluid A interference fringes (Fig. 3a, b). This effect is caused by the tendency of fluid A droplets to collect in between the ridges.

### Friction performance of euplantulae on smooth and microstructured substrates

We measured pushing and pulling forces of single euplantulae on both smooth and microstructured PMMA surfaces. On smooth surfaces, the contact area appeared, under epi-illumination, as a dark zone. On the 1-µm high microstructured substrate, the contact area consisted of zones that were either darker or brighter than the background intensity (Fig. 4b). The darker areas represent zones where the pad makes full contact, both to the pillars and to the surface in between them. The bright areas are areas where the pad is in contact only with the top of the pillars (visible as dark spots) but not with the area in between. The increased intensity of reflected light in this case is explained by the presence of a layer of air between the cuticle and the base of the pillars. Light is reflected not only from the glass
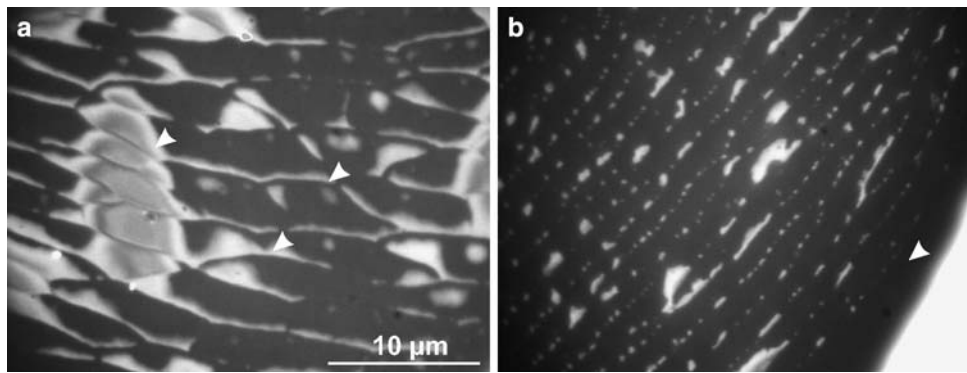
Fig. 3 IRM image of *N. cinerea* euplantulae ridges. **a** Immediately after contact with smooth glass, hydrophilic fluid A droplets become visible in the contact area. The ridges are visible as 'breaks' in the interference pattern of these droplets and small amounts of the fluid collect in channels in between the ridges (see *arrow heads*). **b** After several minutes in contact there is no fluid A directly visible at the edge of the pad (*arrow head*), demonstrating the highly volatile properties of fluid A in contact with air (see Federle et al. 2002)

Fig. 4 **a** SEM of the microstructured rough surface (*tilted view*). **b** Contact area of one euplantula on the 1-μm high microstructured substrate. *Bright zone* indicates that the pad touches only the top of the pillars (*i*), *dark contact area* indicates that the pad makes contact with the area in between the 1-μm high pillars (*ii*)
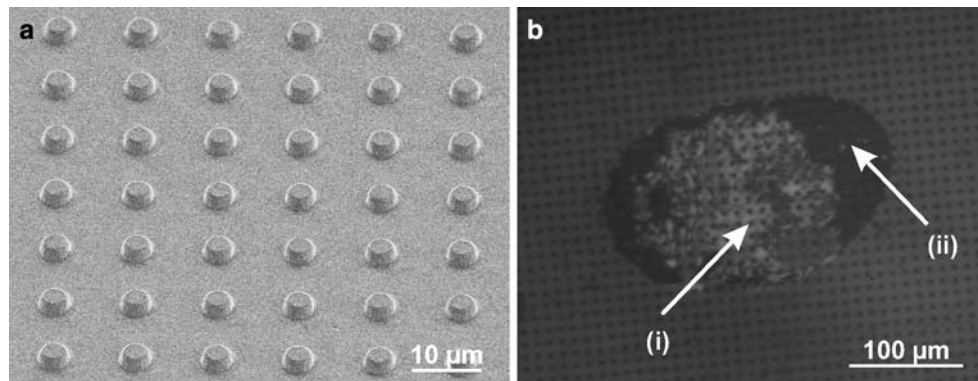
surface but also from the surface of the pad, which may be approximately parallel to it. On the 4-μm high microstructured substrate the contact area consisted only of bright areas (interspersed by dark spots at the pillars), showing that the pads were unable to conform fully to these higher aspect ratio structures.

Rough versus smooth surfaces

For a comparison of the forces produced by euplantulae on different surfaces, we examined pushing slides as the more biologically relevant condition. Measurements for different normal forces produced similar results. Friction force, contact area and shear stress showed significant differences between the three surfaces (Table 1). On the 4-μm high microstructured surface, where euplantulae did not make contact to the bottom of the pillars, both contact area and friction were significantly reduced. Contact area was also reduced in the 1-μm high microstructured surface, but here friction forces were not significantly different from those on the smooth surface (Table 2). As a result, this surface exhibited the highest shear stress, being significantly greater than the shear stress on either the smooth or the 4-μm high microstructured surfaces (Fig. 5; Table 2).

Pushing versus pulling

The effect of pushing and pulling was examined on three different PMMA substrates, a smooth surface, and two microstructured surfaces of 1 and 4 μm height. Varying normal force had an effect on the results obtained for pushing versus pulling. Increases in normal force were associated with increases in friction forces, contact area and shear stress. There was a significant interaction effect between normal force and direction for friction force on the smooth surface as well as for contact area and shear stress on the 4-μm high microstructured surface. Therefore, the effect of direction had to be analysed separately for each normal force.

Despite the significant interaction between normal force and sliding direction, the results obtained for each normal force were similar (Fig. 5). Friction forces were significantly higher for the pulling direction on smooth and 1-μm high microstructured surfaces but there was no significant difference in friction force on the 4-μm high microstructured surface, at either normal force (Table 3). The higher friction force during pulls was mainly explained by a higher contact area.

However, when shear stress was considered, there was no longer a significant difference between pushing and pulling on smooth surfaces at either normal force, nor on the

Table 1 Statistics for one-way repeated measures ANOVA comparing surface types (surface), repeated at two different normal forces (NF), for pushing slides

Friction force (mN)				
Between subjects	MS	df	F	P
Surface	553.130	2	11.850	**<0.001**
Error	46.676	27		
Repeated measures	Wilks' Lambda	df	F	P
Normal force	1.000	1, 27	0.012	0.913
NF × surface	0.877	2, 27	1.897	0.169
Contact area (mm²)				
Between subjects	MS	df	F	P
Surface	3.56×10^{-3}	2	92.529	**<0.001**
Error	3.84×10^{-5}	27		
Repeated measures	Wilks' Lambda	df	F	P
Normal force	0.989	1, 27	0.308	0.583
NF × surface	0.912	2, 27	1.298	0.290
Shear stress (kPa)				
Between subjects	MS	df	F	P
Surface	2.18×10^{7}	2	10.670	**<0.001**
Error	2.04×10^{6}	27		
Repeated measures	Wilks' Lambda	df	F	P
Normal force	0.747	1, 27	9.131	**0.005**
NF × surface	0.850	2, 27	2.390	0.111

P values < 0.05 are shown in bold

1-μm high microstructured surface at 0.5 mN normal force. On the 4-μm high microstructured surface and on the 1-μm high microstructured surface at 1.0 mN normal force, immobilized euplantulae showed a significantly higher shear stress in the pushing direction (Table 3), consistent with the function of the euplantulae during locomotion and the predicted effect of the surface ridges.

Discussion

We have previously shown that the euplantulae of *N. cinerea* are friction pads specialized for pushing (Clemente and Federle 2008). The results of the present study show that on a rough surface the ability of these pads to generate pushing forces is enhanced by the anisotropic nanostructure of its surface. The surface of the euplantulae is covered by lines of asymmetrical ridges ca. 200 nm high, with steep slopes facing distally, but shallower slopes proximally. Such a configuration facilitates interlocking with a rough substrate

when pushed in the distal direction, but the pad slips more easily when pulled proximally.

Direction dependence of tarsal euplantulae in cockroaches

In our previous study, we investigated friction forces of *N. cinerea* euplantulae on smooth surfaces and found that pads generated higher forces in the pushing direction only when the flexible tarsus was left free to move (Clemente and Federle 2008). By contrast, pad forces were higher for pulling on smooth surfaces when the tarsus was fixated, and this result has been confirmed in the present study. Friction forces per unit contact area (shear stress) generated by euplantulae on a smooth surface were also not higher in the pushing direction (Clemente and Federle 2008 and this study). Thus, the natural direction dependence on smooth surfaces is mainly based on changes in contact area resulting from the flexibility of the tarsal chain.

On the microstructured surfaces used in this study, however, the euplantulae performed differently. Shear stress was higher in the pushing than in the pulling direction on the 4-μm high microstructured surface. This can be explained by the interlocking of the anisotropic surface structures of the pad with the pillars of the microstructured surface. This effect was less obvious on the 1-μm high microstructured surface, which can be explained by the difference in contact formation of the euplantulae during the slide. On the 4-μm high microstructured surface, the pad made only contact to the top of the pillars, but full contact was observed on the 1-μm high microstructured surface (although on a smaller area than on the smooth surface). The complete contact probably gives rise to a greater adhesive contribution to friction forces. The adhesion-induced friction forces are likely to be the same in both the distal and proximal direction; and this effect may mask the smaller effect of interlocking. Therefore, the direction dependence of the ridges is more visible when the adhesive contact is reduced.

Despite the interlocking of the nanostructures, we observed a gradual sliding of the pads on the rough substrate. This finding is probably of biological significance, because it suggests that the euplantulae are designed to avoid excessive peak forces and stick-slip, both of which would result in increased wear of the pad. It is possible that the small length scale of the surface ridges gives rise to very small stick-slip movements of the pad that are too small to be observed using our setup. Due to the softness of the euplantula cuticle, it is more likely that individual interlocking ridges fail independently of each other, thereby resulting in a steady movement of the whole pad. Moreover, the presence of fluid secretion in the euplantula contact zone probably results in some lubrication that further reduces excessive forces and wear (Drechsler and Federle

Table 2 Summary of the surface effects presented in Table 1

Comparison	0.5 mN normal force		1.0 mN normal force	
	Mean diff $\pm$ SE	Post hoc test	Mean diff $\pm$ SE	Post hoc test
Friction force (mN)				
Smooth versus 1 μm	-4.31 ± 2.04	$q = 2.11, P = 0.147$	-0.87 ± 1.434 '	$q = 0.61, P = 0.671$
Smooth versus 4 μm	7.26 ± 1.84	$q = 3.95, P = \mathbf{0.010}$	7.49 ± 1.29	$q = 5.78, P < \mathbf{0.001}$
1 versus 4 μm	11.5 ± 1.96	$q = 5.90, P = \mathbf{0.001}$	8.36 ± 1.38	$q = 6.06, P = \mathbf{0.001}$
Contact area (mm² × 10⁻³)				
Smooth versus 1 μm	19.0 ± 2.16	$q = 8.77, P < \mathbf{0.001}$	23.2 ± 1.17	$q = 19.8, P < \mathbf{0.001}$
Smooth versus 4 μm	22.9 ± 1.96	$q = 11.7, P < \mathbf{0.001}$	25.5 ± 1.06	$q = 24.1, P < \mathbf{0.001}$
1 versus 4 μm	3.96 ± 2.09	$q = 1.89, P = 0.191$	2.29 ± 1.13	$q = 2.04, P = 0.161$
Shear stress (kPa)				
Smooth versus 1 μm	-1911 ± 275	$q = 6.95, P < \mathbf{0.001}$	$-2{,}459 \pm 413$	$q = 5.94, P = \mathbf{0.001}$
Smooth versus 4 μm	-503 ± 248	$q = 2.03, P = 0.163$	-857 ± 373	$q = 2.29, P = 0.116$
1 versus 4 μm	$1{,}408 \pm 264$	$q = 5.32, P = \mathbf{0.001}$	$1{,}601 \pm 398$	$q = 4.02, P = \mathbf{0.008}$

Student–Newman–Keuls post hoc tests showing the groups being compared, the mean difference and its standard error, as well as the q statistic and probability level for each comparison. Post hoc tests are shown separately for each normal force. P values < 0.05 shown in bold

Contact area (mm² × 10⁻³) note: the table header for contact area is rendered above.

2006). Similar results have been shown in biomimetic adhesive systems. Microstructured surfaces with mushroom-shaped or hexagonal pillars also did not exhibit stick-slip, unlike smooth surfaces of the same material (Varenberg and Gorb 2007; Varenberg and Gorb 2009). However, when lubricated with fluid, even smooth surfaces did not show stick-slip behaviour (Varenberg and Gorb 2009).

The high pulling force of the euplantulae on the smooth surface seems to contradict a specialization of these organs for pushing. However, since the tarsal segments were completely immobilized in the present study, they were unable to peel away from the surface as it would happen under natural conditions when the tarsus is free to move (Clemente and Federle 2008).

The higher shear stress of the immobilized euplantulae on the 1-μm high microstructured surface may primarily result from the "rubbery" friction of the pad. When the soft pad slides across the rough substrate, the surface pillars will exert oscillating forces on the pad, leading to periodic deformation and energy dissipation within the pad material (Grosch 1963; Persson 1998). The higher shear stress may also partly result from an underestimation of contact area. On the 1-μm high microstructured surface, the pad cuticle may also make contact to the sides of the pillars, so that the actual contact area is larger than the measured one.

Function of surface microstructures in adhesive pads

Microstructured surfaces of adhesive pads have been observed in many insects (Gorb et al. 2000; Beutel and Gorb 2001; Schulmeister 2003; Beutel and Gorb 2006) and vertebrates (Green 1981; Smith et al. 2006; Barnes 2007). Several possible biological functions have been proposed for these surface patterns. First, surface patterns on adhesive pads might enhance their ability to deform and make

contact to rough substrates (Scholz et al. 2009). Second, microstructured surfaces of adhesive pads could facilitate fluid drainage (Federle et al. 2006; Persson 2007b). Excessive fluid in the adhesive contact zone (which could be both water present on wet surfaces or pad secretion) reduces both adhesion and friction forces (Drechsler and Federle 2006; Bullock et al. 2008). The IRM images suggest that the ridges on the surface of the euplantulae of *N. cinerea* could assist in draining fluid secretion from the contact zone. A third possible benefit of microstructured adhesive surfaces is that they can arrest "cracks" propagating through the contact zone, because the elastic energy released at the crack tip during peeling is not transferred to the zone ahead of it and is therefore lost. This increases the work of adhesion and thus the force needed to peel off the pad. Enhanced adhesion via crack trapping has been demonstrated in artificial model systems by several authors (Jagota and Bennison 2002; Ghatak et al. 2004; Hui et al. 2004; Chung and Chaudhury 2005; Glassmaker et al. 2005; Chan et al. 2008).

While surface patterns on smooth attachment pads may have one or several of the above functions, the stepped surface microstructures on the euplantulae of *N. cinerea* may be primarily important for interlocking with rough substrates. Many studies have shown both theoretically and empirically that adhesion of smooth adhesives is reduced on rough surfaces (Fuller and Tabor 1975; Kendall 2001; Persson and Gorb 2003; Peressadko et al. 2005; Gorb 2008). Therefore, the microstructured surfaces of cockroach euplantulae may reduce this effect by combining the advantages of adhesion and interlocking on rough surfaces. The change of orientation of the ridges from the midline to the lateral sides of the euplantulae suggests that the surface pattern also stabilizes the pad against sliding in the lateral (transversal) direction. Although insects keep ground reaction force vectors approxi-
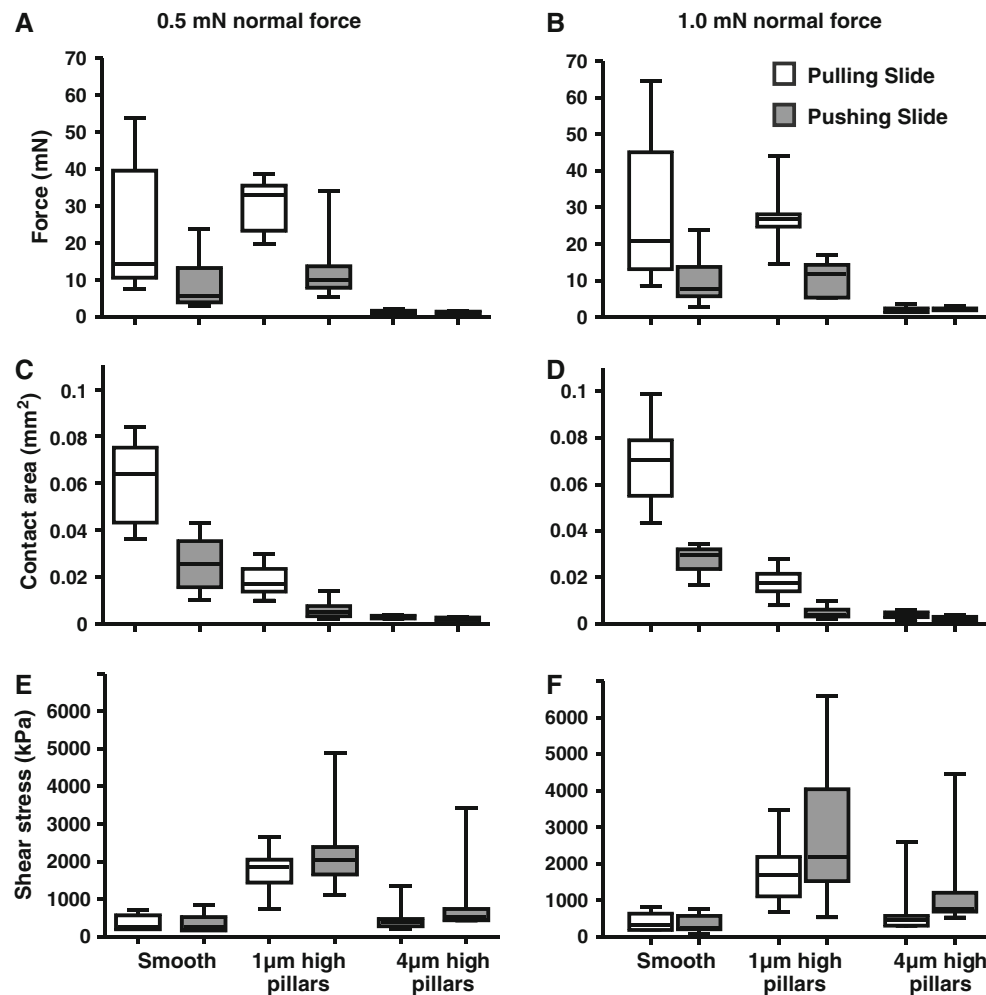
Fig. 5 Friction force (**a**, **b**), contact area (**c**, **d**) and shear stress (**e**, **f**) of *N. cinerea* euplantulae for pushing and pulling on smooth and microstructured surfaces. Results are shown for a normal force of 0.5 mN (**a**, **c**, **e**) and 1.0 mN (**b**, **d**, **f**). *White boxes* indicate a pull, *grey boxes* indicate a push. *Centre lines* and *boxes* represent the median within the 25 and 75% percentiles. *Whiskers* represent the maximum and minimum values

mately aligned along the legs to minimize joint torques (Full et al. 1991), producing significant transverse forces may in some cases be important, e.g. in middle legs during upward or downward climbing. As for pushing, resisting transverse forces with an attachment structure at the tip of the tarsus would be difficult due to the instability of the tarsus. Thus, the proximal tarsus may be better suited both for pushing and for generating transverse forces.

It is still unclear how widespread anisotropic surface patterns are amongst climbing pads of other animals. Many groups possess distally directed hairs or bristles on the ventral surface of the tarsus (e.g. Hymenoptera, Schulmeister 2003). These hairs are probably direction-dependent only on rough surfaces and provide higher friction in the pushing direction by interlocking. The cockroach euplantulae appear to have evolved a design that combines adhesion and interlocking, which might be beneficial for running on surfaces with varying degrees of roughness.

Many of the micro- and nanostructures described for the smooth pads of tree frogs and insects are hexagonal or consist of longitudinal or transversal lines and microfolds; they do not seem to have any obvious direction dependence (Beutel and Gorb 2001). Surface patterns have been mainly studied for distal pads which may be specialized for adhesive function. However, much less information is available for pads on the proximal tarsus, which may be primarily adapted for pushing (but see Schulmeister 2003). Further comparative work is needed to investigate whether anisotropic surface patterns are characteristic features of proximal friction pads.

Microstructured substrates as a tool to study biological adhesion

We believe that the techniques used here to characterize the frictional properties of the euplantulae of cockroaches, will

Table 3 Statistics comparing pushing versus pulling slides, on three different surface types, at two normal forces

Surface	0.5 mN normal force	1.0 mN normal force
Proximal (pulling) slides versus distal (pushing) slides (paired *t* tests)		
Smooth		
Friction force	$t_9 = 4.45$, $P = \textbf{0.002}$	$t_9 = 4.28$, $P = \textbf{0.002}$
Contact area	$t_9 = 10.2$, $P < \textbf{0.001}$	$t_9 = 9.50$, $P < \textbf{0.001}$
Shear stress	$t_9 = 0.09$, $P = 0.931$	$t_9 = 0.99$, $P = 0.347$
1-µm high microstructured surface		
Friction force	$t_7 = 5.93$, $P = \textbf{0.001}$	$t_7 = 7.11$, $P < \textbf{0.001}$
Contact area	$t_7 = 5.01$, $P = \textbf{0.002}$	$t_7 = 6.59$, $P < \textbf{0.001}$
Shear stress	$t_7 = 1.45$, $P = 0.190$	$t_7 = 2.39$, $P = \textbf{0.048}$
4-µm high microstructured surface		
Friction force	$t_{11} = 0.77$, $P = 0.458$	$t_{11} = 1.43$, $P = 0.180$
Contact area	$t_{11} = 3.81$, $P = \textbf{0.003}$	$t_{11} = 5.65$, $P < \textbf{0.001}$
Shear stress	$t_{11} = 2.31$, $P = \textbf{0.041}$	$t_{11} = 3.88$, $P = \textbf{0.003}$

The effect of pushing versus pulling was analysed separately for each normal force. P values <0.05 shown in bold

greatly enhance the study of the interaction of biological attachment systems with rough substrates. It has the advantage that (1) the surface "roughness" is well defined and has a controllable length scale, (2) the microstructured substrates are transparent and allow the adhesive contact area to be measured and thus adhesive and shear stresses to be quantified, and that (3) the chemical nature of the surface can be tailored by choosing a large number of transparent polymers with different properties.

We used this technique to provide evidence for direction-dependent friction, and interlocking of the tarsal pads of the cockroach *N. cinerea*, on rough surfaces, which is likely the result of the anisotropic, microstructured surface of the euplantulae. The study of biological attachment systems may have important implications for the development of biomimetic structures that are capable of creating friction on both smooth and rough surfaces. The direct measurement of shear stress on rough surfaces with transparent, microstructured substrates is to our knowledge novel, and this technique may advance our understanding of biological adhesion on rough surfaces.

References

Barbero DR, Saifullah MSM, Hoffmann P, Mathieu HJ, Anderson D, Jones GAC, Welland ME, Steiner U (2007) High resolution nanoimprinting with a robust and reusable polymer mold. Adv Funct Mater 17:2419–2425

Barnes WJP (2007) Functional morphology and design constraints of smooth adhesive pads. MRS Bull 32:479–485

Betz O (2002) Performance and adaptive value of tarsal morphology in rove beetles of the genus *Stenus* (Coleoptera, Staphylinidae). J Exp Biol 205:1097–1113

Beutel RG, Gorb SN (2001) Ultrastructure of attachment specializations of hexapods (Arthropoda): evolutionary patterns inferred from a revised ordinal phylogeny. J Zool Syst Evol Res 39:177–207

Beutel RG, Gorb SN (2006) A revised interpretation of attachment structures in Hexapoda with special emphasis on Mantophasmatodea. Arthropod Syst Phylogeny 64:3–25

Bullock JMR, Federle W (2009) Division of labour and sex differences between fibrillar, tarsal adhesive pads in beetles: effective elastic modulus and attachment performance. J Exp Biol 212:1878–1888

Bullock JMR, Drechsler P, Federle W (2008) Comparison of smooth and hairy attachment pads in insects: friction, adhesion and mechanisms for direction-dependence. J Exp Biol 211:3333–3343

Busscher HJ, Van Pelt AWJ, De Boer P, De Jong HP, Arends J (1984) The effect of surface roughening of polymers on measured contact angles of liquids. Colloids Surf 9:319–331

Chan EP, Smith EJ, Hayward RC, Crosby AJ (2008) Surface wrinkles for smart adhesion. Adv Mater 20:711–716

Chung JY, Chaudhury MK (2005) Roles of discontinuities in bio-inspired adhesive pads. J R Soc Interface 2:55–61

Clemente CJ, Federle W (2008) Pushing versus pulling: division of labour between tarsal attachment pads in cockroaches. Proc R Soc Lond B Biol Sci 275:1329–1336

Dai Z, Gorb SN, Schwarz U (2002) Roughness-dependent friction force of the tarsal claw system in the beetle *Pachnoda marginata* (Coleoptera, Scarabaeidae). J Exp Biol 205:2479–2488

Drechsler P, Federle W (2006) Biomechanics of smooth adhesive pads in insects: influence of tarsal secretion on attachment performance. J Comp Physiol A 192:1213–1222

Endlein T, Federle W (2008) Walking on smooth or rough ground: passive control of pretarsal attachment in ants. J Comp Physiol A 194:49–60

Federle W, Riehle M, Curtis ASG, Full RJ (2002) An integrative study of insect adhesion: mechanics and wet adhesion of pretarsal pads in ants. Integr Comp Biol 42:1100–1106

Federle W, Barnes WJP, Baumgartner W, Drechsler P, Smith JM (2006) Wet but not slippery: boundary friction in tree frog adhesive toe pads. J R Soc Interface 3:689–697

Frazier SF, Larsen GS, Neff D, Quimby L, Carney M, DiCaprio RA, Zill SN (1999) Elasticity and movements of the cockroach tarsus in walking. J Comp Physiol A 185:157–172

Full RJ, Blickhan R, Ting LH (1991) Leg design in hexapedal runners. J Exp Biol 158:369–390

Fuller KNG, Tabor D (1975) The effect of surface roughness on the adhesion of elastic solids. Proc R Soc Lond A 345:327–342

Ghatak A, Mahadevan L, Yun J, Chaudhury M, Shenoy V (2004) Peeling from a biomimetically patterned thin elastic film. Proc R Soc Lond A 460:2725–2735

Glassmaker NJ, Jagota A, Hui C-Y (2005) Adhesion enhancement in a biomimetic fibrillar interface. Acta Biomater 1:367–375

Gorb S (2001) Attachment devices of insect cuticle. Kluwer, Dordrecht

Gorb SN (2008) Smooth attachment devices in insects. In: Casas J, Simpson SJ (eds) Advances in insect physiology, vol 34. Academic Press, London, pp 81–116

Gorb S, Jiao Y, Scherge M (2000) Ultrastructural architecture and mechanical properties of attachment pads in *Tettigonia viridissima* (Orthoptera Tettigoniidae). J Comp Physiol A 186:821–831

Gorb S, Gorb E, Kastner V (2001) Scale effects on the attachment pads and friction forces in syrphid flies. J Exp Biol 204:1421–1431

Green DM (1981) Adhesion and the toe pads of tree frogs. Copeia 1981:790–796

Grosch KA (1963) The relation between the friction and visco-elastic properties of rubber. Proc R Soc Lond A 274:21–39

Huber G, Gorb SN, Hosoda N, Spolenak R, Arzt E (2007) Influence of surface roughness on gecko adhesion. Acta Biomater 3:607–610

Hui CY, Lin YY, Baney JM, Kramer EJ (2001) The mechanics of contact and adhesion of periodically rough surfaces. J Polym Sci B Polym Phys 39:1195–1214

Hui C-Y, Glassmaker NJ, Tang T, Jagota A (2004) Design of biomimetic fibrillar interfaces: 2. Mechanics of enhanced adhesion. J R Soc Interface 1:35–48

Hui C-Y, Glassmaker NJ, Jagota A (2005) How compliance compensates for surface roughness in fibrillar adhesion. J Adhes 81:699–721

Jagota A, Bennison SJ (2002) Mechanics of adhesion through a fibrillar microstructure. Integr Comp Biol 42:1140–1145

Jiao Y, Gorb S, Scherge M (2000) Adhesion measured on the attachment pads of *Tettigonia viridissima* (Orthoptera, Insecta). J Exp Biol 203:1887–1895

Jones RAL, Richards RW (1999) Polymers at surfaces and interfaces. Cambridge University Press, Cambridge

Kendall K (2001) Molecular adhesion and its applications. Kluwer, Dordrecht

Kim TW, Bhushan B (2007) Adhesion analysis of multi-level hierarchical attachment system contacting with a rough surface. J Adhes Sci Technol 21:1–20

Lees AD, Hardie J (1988) The organs of adhesion in the aphid *Megoura viciae*. J Exp Biol 136:209–228

Peressadko AG, Hosoda N, Persson BNJ (2005) Influence of surface roughness on the adhesion between elastic bodies. Phys Rev Lett 95:124301–124304

Persson BNJ (1998) On the theory of rubber friction. Surf Sci 401:445–454

Persson BNJ (2007a) Biological adhesion for locomotion on rough surfaces: basic principles and a theorist's view. MRS Bull 32:486–490

Persson BNJ (2007b) Wet adhesion with application to tree frog adhesive toe pads and tires. J Phys Condens Matter 19:376110

Persson BNJ, Gorb S (2003) The effect of surface roughness on the adhesion of elastic plates with application to biological systems. J Chem Phys 119:11437–11444

Roth LM, Willis ER (1952) Tarsal structure and climbing ability of cockroaches. J Exp Zool 119:483–517

Russell TP (1990) X-ray and neutron reflectivity for the investigation of polymers. Mater Sci Rep 5:171–271

Santos R, Gorb S, Jamar V, Flammang P (2005) Adhesion of echinoderm tube feet to rough surfaces. J Exp Biol 208:2555–2567

Scherge M, Gorb SN (2001) Biological micro- and nanotribology: nature's solutions. Springer, Berlin

Scholz I, Barnes WJP, Smith JM, Baumgartner W (2009) Ultrastructure and physical properties of an adhesive surface, the toe pad epithelium of the tree frog, Litoria caerulea White. J Exp Biol 212:155–162

Schulmeister S (2003) Morphology and evolution of the tarsal plantulae in Hymenoptera (Insecta), focussing on the basal lineages. Zool Scr 32:153–172

Smith JM, Barnes WJP, Downie JR, Ruxton GD (2006) Structural correlates of increased adhesive efficiency with adult size in the toe pads of hylid tree frogs. J Comp Physiol A 192:1193–1204

Spagna JC, Goldman DI, Lin P, Koditschek DE, Full RJ (2007) Distributed mechanical feedback in arthropods and robots simplifies control of rapid running on challenging terrain. Bioinspir Biomim 2:9–18

Stork NE (1980) Experimental analysis of adhesion of *Chrysolina polita* (Chrysomelidae: Coleoptera) on a variety of surfaces. J Exp Biol 88:91–107

Varenberg M, Gorb S (2007) Shearing of fibrillar adhesive microstructure: friction and shear-related changes in pull-off force. J R Soc Interface 4:721–726

Varenberg M, Gorb SN (2009) Hexagonal surface micropattern for dry and wet friction. Adv Mater 21:483–486

Voigt D, Schuppert JM, Dattinger S, Gorb SN (2008) Sexual dimorphism in the attachment ability of the Colorado potato beetle *Leptinotarsa decemlineata* (Coleoptera: Chrysomelidae) to rough substrates. J Insect Physiol 54:765–776